

THE DESIGN OF ADJUSTABLE RADIO FREQUENCY FILTER (RF) BY USING MICROSTRIP LINE TECHNOLOGY

Sadjad Divandari,

*Department of Electrical Engineering, K.N. Toosi University of Technology, Tehran, Iran.
sadjad.divandari@ee.kntu.ac.ir*

Seyed Abdullah Mirtaheeri,

*Department of Electrical Engineering, K.N. Toosi University of Technology, Tehran, Iran.
Mirtaheeri@eed.kntu.ac.ir*

Abstract. Nowadays, filters are the main component of communication systems. Often they are used to select certain frequencies. Filters usually play a key role in choosing or limiting the radio frequency signals. Compressed midrange filters are constructed by using in-line digital microstrip lines on composite lenses suitable for high frequencies with over 6,000 sub-layers. BFP microstrips, 1.69 / 2.3GHz dual-state dual-band 1.69 / 2.3GHz, are the new generation of microstrips that have just been introduced. In the present study, the performance of this type of microstrip was simulated. To simulate the BFP efficiency with different makeups, a set of simulations was performed based on HFSS. After examining a few cases, the study of the relationship between different parameters has been investigated. Finally, after examining different modes, the conclusions were discussed. The proposed filter design method can be very suitable for designing the receiver module and compact transmitter.

Keywords: microstrip, radio filter, intermediate frequency band pass filter, biaxial filter and double-sided.

Introduction. Intermediate frequency band pass filters are an electronic component that allows the passage of signals in a specific range and does not pass frequencies beyond the specified range. With the rapid growth of radio systems, wireless systems, communication devices, the use of cross-pass microstrip filters, etc. has also been accompanied by dramatic growth [1]. Many communication systems have a complex structure; hence there is a need for small circuit design, low cost, high efficiency, easy assembly, and multi-frequency capability. That's why there are a variety of filter designs and patterns that are designed based on various parameters such as Butterworth, Chebyshev and Elliptic filters, or in terms of bandwidth such as broadband or dual-bandwidth. Two-band filters generally use for applications in which two different signals with different frequency ranges which are required to pass at a time [2]. Bandwidth filters are also used in applications that require a wide range of frequencies to pass across a spectrum. For example, microsphere filters are widely used for radio frequencies and microwave systems [3]. For this reason, the size of the filter is one of the most important concerns that should be considered in design. The filter must be designed in such a way as to ensure that it is embedded in electronic equipment. In addition, filter losses play an important role because it affects the filter efficiency [1].

High-efficiency multi-pass filters are ideal for the generation of communication systems, especially wireless systems, in the radio frequency band. The most commonly used method of designing multiband filters is based on the base load resonator [3-1] or stepped impedance resonator [6-4]. However, there are other ways to implement a multi-band filter, which is used to combine different resonators to achieve multi-band filtering [8,7]. For example, a multi-band BFP can be obtained from a pass filter and an interlaced filter [9]. But the main problem with these methods is the large size of the final structure because it uses a large number of resonators. Also, the degree of freedom in the design of each passing band is not enough. The calm wave resonators do not work well for most bandwidths, although they provide a great response to bandwidth. Multi-layered structures have many drawbacks, such as complexity of makeup and structural problems. At the same time, stacked elements may not always be operational. The use of parallel-coupled micro-strips due to the plate structure and simple design is one of the common types of filters for RF systems [11,10]. The main purpose of this study is to investigate the properties of microstrip intermediate filters and design a two-band two-state microstrip filter using simulation by HFSS software. The filter design is of a binary type and two-band type and has a resonant frequency range of 1 to 5 GHz. As discussed earlier, this issue has already been less widely considered.

1.1 Filter-based equations

For radio frequency applications, the spatial distribution parameter (S_{21}) is used to determine the transfer function. In many applications, instead of S_{21} , the second power S_{21}^2 is used.

$$1 - |S_{21}(\Omega)|^2 = \frac{1}{1 + \epsilon^2 F_n^2(\Omega)}$$

In the above equation, ϵ denotes the wavelet constant, $F_n(\Omega)$ is the filter function and Ω is the frequency variable. If the transfer function is a given, the filter losses are calculated as follows:

$$3(\text{dB}) = 10 \log[1 - |S_{21}(\Omega)|^2]$$

Designed filters using the Butterworth approximation in the passband, the most characteristic is flatness. In Figure 1, the Butterworth filter attenuation characteristics of the low pass can be shown.

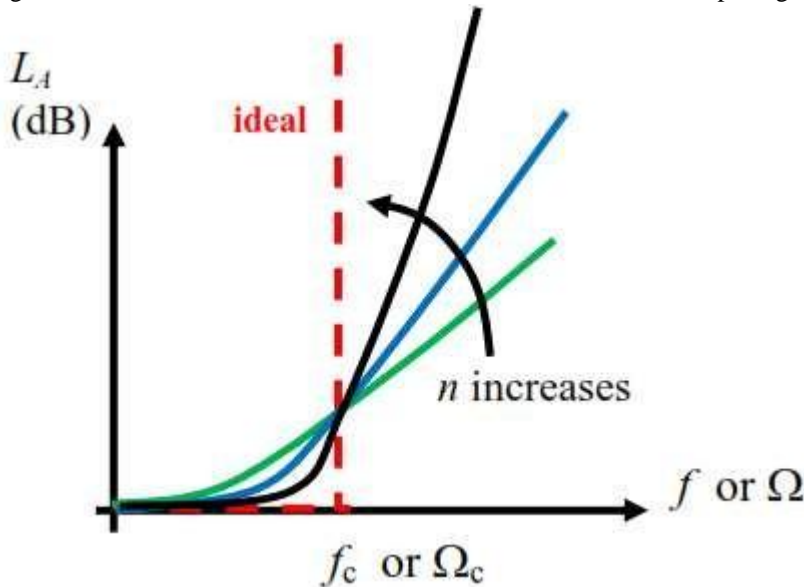


Figure 1. Butterworth curve filter characteristic

In the passband area $f < f_c$, the attenuation of the low pass filter is ideal at 0dB. This approximation is often appropriate from the frequency 0 Hz to the cutoff frequency indicated by the symbol f_c . For area $f > f_c$ for ideal lowpass filter $L_A \rightarrow \infty$.

In this case, the square of the size of the transfer function is calculated as follows:

$$|H(\Omega)|^2 = \frac{1}{1 + \Omega^{2n}}$$

Figure 2 shows the filter implementation circuit by using the central components such as inductor (L) and capacitor (C) for the degree of individual freedom and the filter pair (N). Butterworth's approximation for filter design is used in situations where attenuation at a frequency $\Omega = \Omega_c = 1$ is equal to 3dB. Therefore, the following relationships can be used to obtain the values of L and C in the circuit:

$$\begin{aligned} g_0 &= g_{n+1} = 1 \\ g_k &= 2 \sin\left(\frac{(2k-1)\pi}{2n}\right), \quad k = 1, 2, \dots, n \end{aligned}$$

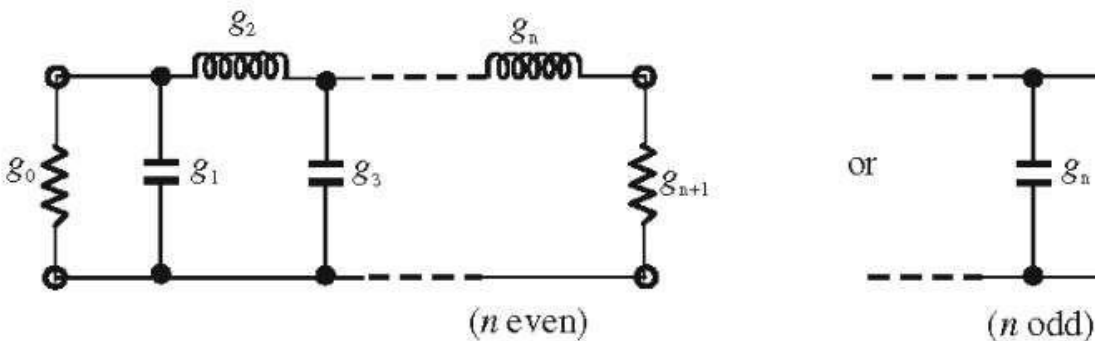


Figure 2. Conceptual concept of the filter using LC components

The amount of N can be obtained by using the additional constraints raised in the problem. For example, one of these limitations is to have a minimum coefficient of attenuation coefficient at a critical frequency. In practical applications, casualties in the transit area are typically more than zero. Approximation of Chebyshev is based on this feature. These values can range from 0.01 to 0.1dB and even slightly more. The Chebyshev approximation shows that some waves in the passband can lead to a greater slope in the passband. Figure (3) shows the damping characteristic for a low pass filter based on the Chebyshev approximation.

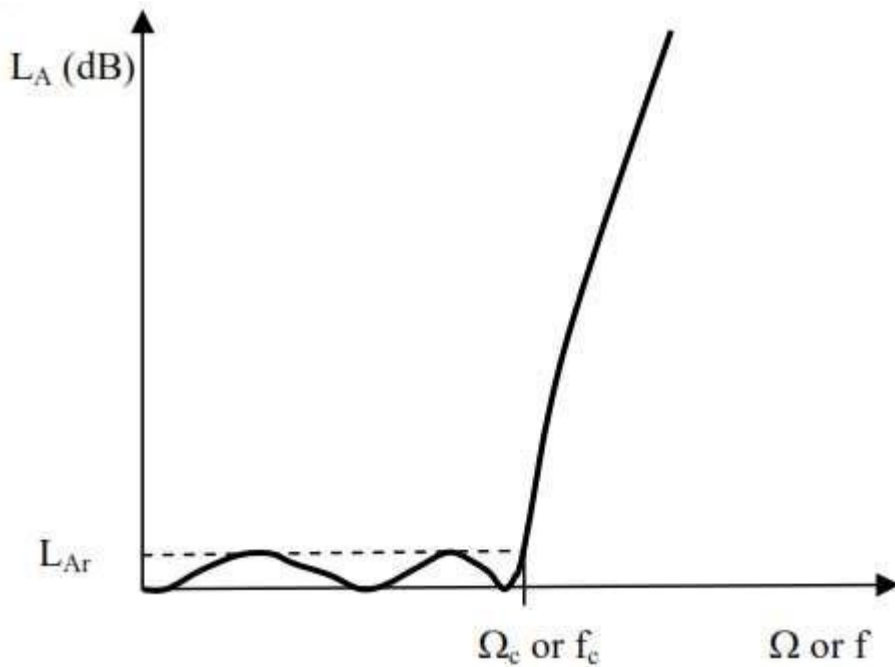


Figure 3 Attenuation characteristic for low pass filter using Chebyshev approximation

The second square of the size of the transfer function is calculated using the Chebyshev approximation as follows:

$$|T_n(\Omega)|^2 = \frac{1}{1 + \epsilon^2 T_n^2(\Omega)}$$

In the above relation, $T_n(\Omega)$ is the Chebyshev function of the first type without N degree.

The values of different components can be calculated by using the following rules:

$$T_0(\Omega) = 1$$

$$T_1(\Omega) = \cos(\Omega)$$

$$T_2(\Omega) = 2\cos^2(\Omega) - 1$$

$$T_3(\Omega) = 4\cos^3(\Omega) - 3\cos(\Omega)$$

$$T_4(\Omega) = 8\cos^4(\Omega) - 8\cos^2(\Omega) + 1$$

The material provided for implementation of lowpass filters is valid. To review intermediate filters, it is necessary to consider the characteristics of these filters.

Transitionally, the component L turns into a series of combinations of L_s and C_s while component C converts to the parallel combination L_p and C_p . If the cut off frequencies are represented by ω_1 and ω_2 , the relative frequency bandwidth is calculated as follows:

$$\omega = \sqrt{\frac{\omega_2}{\omega_1}}$$

The amount for new components is calculated as follows.

To combine the series can be written:

$$Z = \frac{1}{\frac{1}{Z_1} + \frac{1}{Z_2}}$$

$$Y = \frac{1}{Z}$$

It can also be written for parallel composition:

$$Y = \frac{1}{Z_1} + \frac{1}{Z_2}$$

$$= \left(\frac{1}{Z_0} \right)^{-0} \quad)17($$

In the above relations, Z_0 represents the load Impedance, which is assumed in most practical applications equal to 50 ohms.

1. Filter concept using microstrip technology:

The microstrip transmission line is most commonly used for the screen transmission line at the radio frequency. The same can be achieved using various methods. For example, using frequency photolithography or thin film technology and thick film. Like other radio frequency transmission lines, the microstrip can be used to design specific components such as filters, transformers, or power dividers. If the microstrip transmission line, as shown in Fig. 4, is used, it is used to transmit the wave using a relatively low frequency, the type of wave propagated in the TEM wave-like waveform. This is the basic mode in the microstrip transmission line.

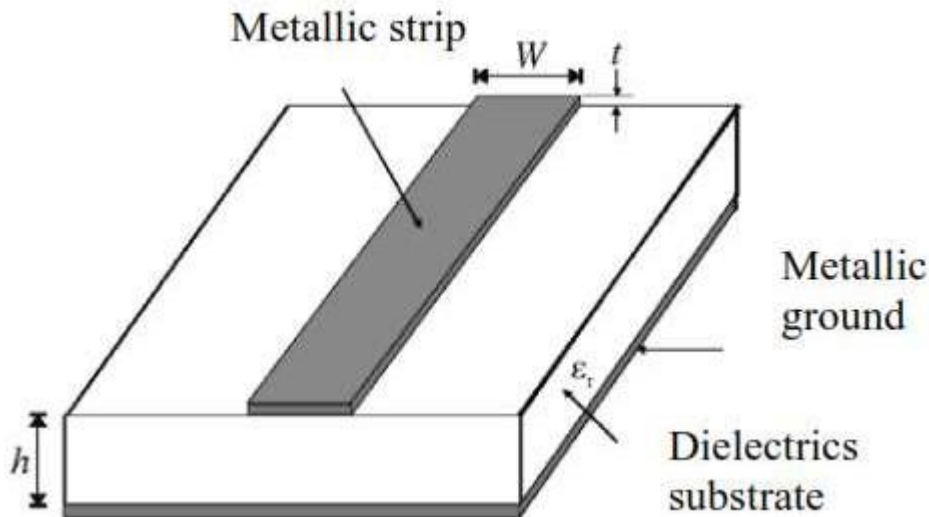


Figure 4. Microstrip transmission line

The width of the strip, represented by the symbol W , along with the dielectric constant and the substrate thickness, determines the impedance characteristic Z_0 for the line. In Figure 5, a parallel coupling filter structure can be seen. In this type of filter, the strips are placed in parallel and in close proximity. The governing equations for the filter are written as follows:

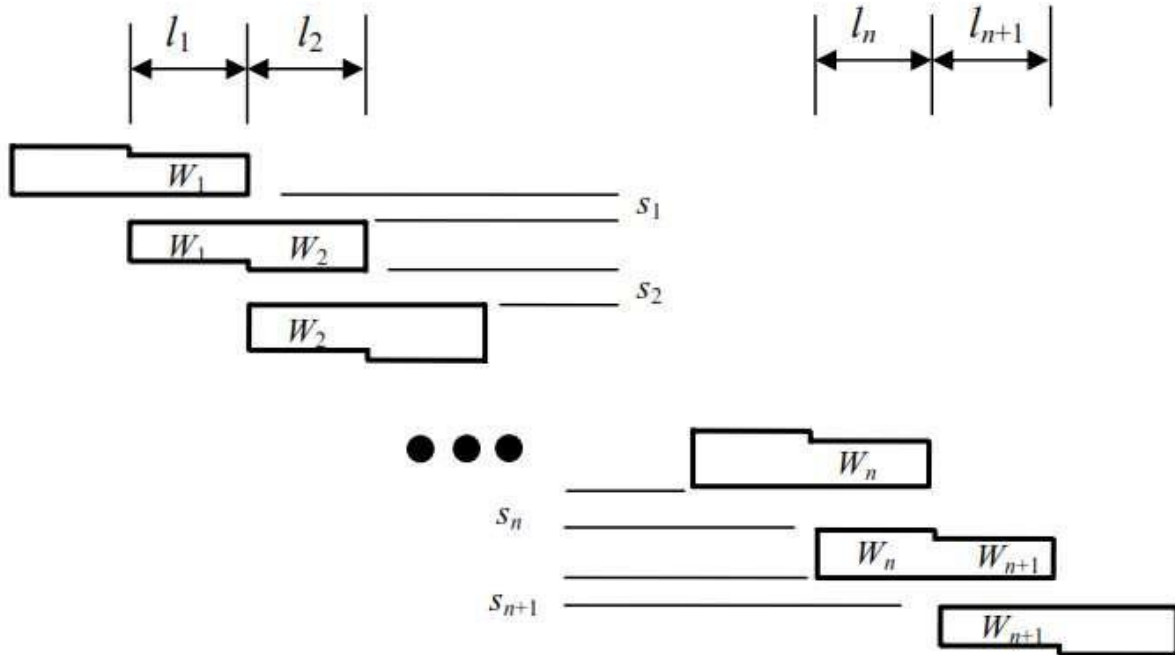


Figure 5. Parallel Couple Pass-through Filter

$$\begin{aligned}
)18 \left(\frac{g_0}{g_1} = \sqrt{\frac{2g_0}{g_1}} \right) \\
)19 \left(\frac{g_{j+1}}{g_j} = \frac{1}{2 \sqrt{g_{j+1}}} \right) \quad j=1, \dots, n-1 \\
)20 \left(\frac{g_{j+1}}{g_j} = \sqrt{\frac{2g_{j+1}}{g_j}} \right)
 \end{aligned}$$

The constants g_0, g_1, \dots, g_n can be derived from existing tables. The FBW is the relative bandwidth described earlier. $J_{j,j+1}$ is the characteristic of the U-turn of the U-transformation, and Y_0 represents the characteristic of the connecting transmission line's edits. With the data of the characteristics of the inductance inverter, one can calculate the characteristic of the coupled mode impedance and the individual mode of the parallel transmission microstrip transmission line as follows:

$$\begin{aligned}
)21 \left(\frac{C_{j,j+1}}{C_0} = \frac{1}{g_0} \left[1 + \frac{g_{j+1}}{g_0} + \left(\frac{g_{j+1}}{g_0} \right)^2 \right] \right) \\
)21 \left(\frac{C_{j,j+1}}{C_0} = \frac{1}{g_0} \left[1 + \frac{g_{j+1}}{g_0} + \left(\frac{g_{j+1}}{g_0} \right)^2 \right] \right) \quad j=0, \dots, n
 \end{aligned}$$

2. Numerical simulation

The dimensions of the cross-pass filter designed in this article are 40×30 [mm] $\wedge 2$ ($L_1 \times W_1$), which is made on a Ruroid 6006 with a thickness of 0.635mm and its dielectric constant of 6.15. In Fig. 6, this is obvious that an exponential between the two-band dual-band filter of the study in this study is observed.

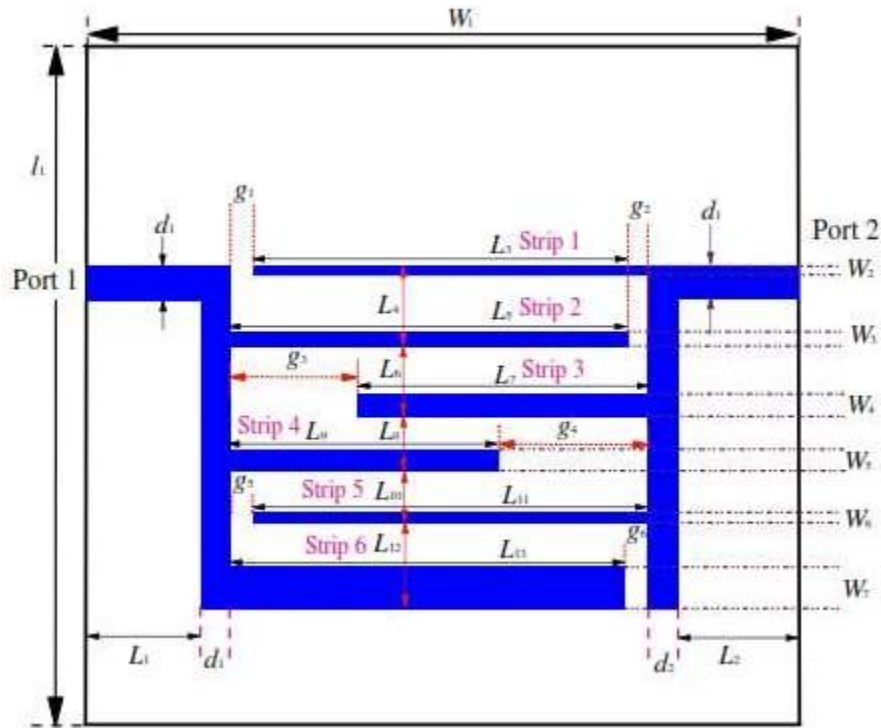


Figure 6. The top view of the two-band two-band intermediate pass filter examined in this study For simulation software HFSS is used.

3. Validation of numerical simulation

To validate the simulation of numerical data, the present study is based on experimental data presented by Emad [12] has been compared. The variations of S_{11} and S_{21} values for the two-band transient cross-pass filter for different frequency values are shown in Figure 7.

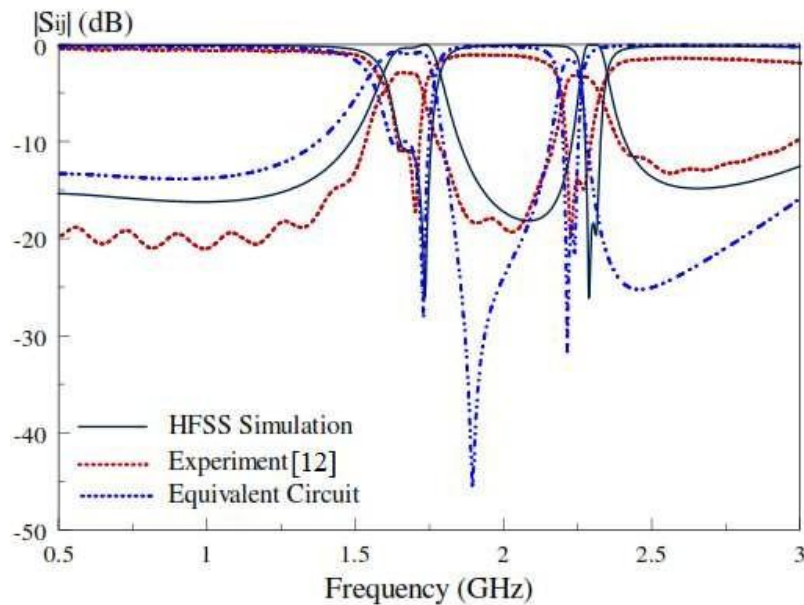


Figure 7. The circuit measured and simulated S_{11} and S_{21} for dual-mode binary filter Figure 7 shows the recurrent, simulated, and measured losses empirically. The lowest error rate is 1.69GHz, in which numerical and experimental data are about 2.07% and the most error is about 9.09%.

4. Numerical results

In this section, the effect of the distance parameter for different samples on the filter performance is investigated. For this purpose, the effect of the parameter changes for the frequency range of 0.5 to 3GHz will be investigated. The effect of the distance on the first test sample is shown in Figs. (8) to (24).

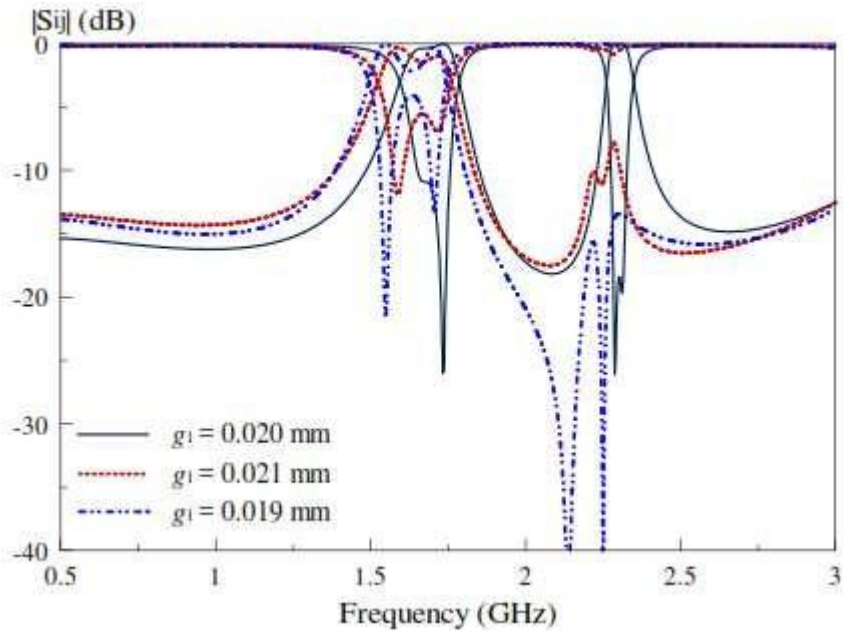


Figure 8. The first response to the sample
As can be seen in figure (8), the passage of the second passage is worse, how much the distance of the gap increases or decreases.

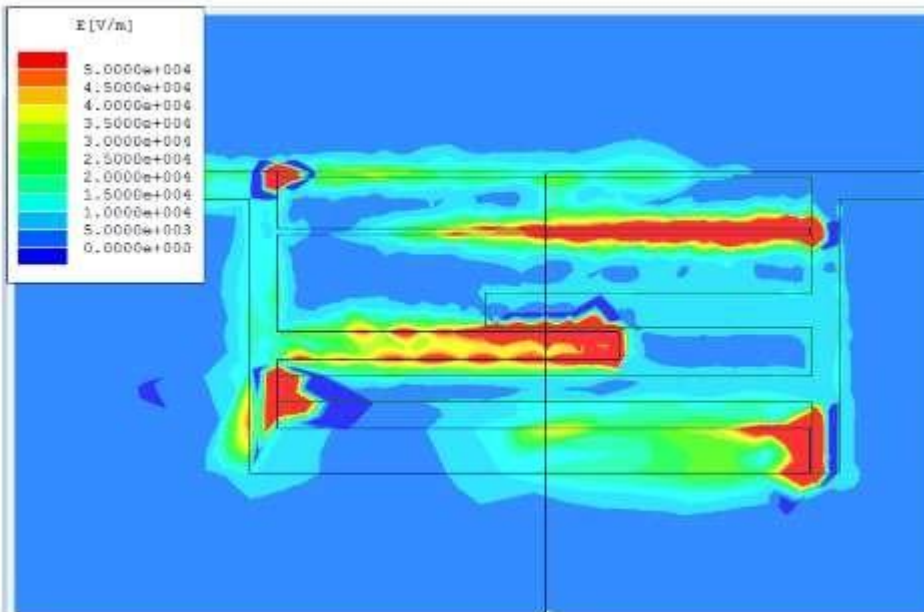


Figure 9. Electric field for $g_1 = 0.021\text{mm}$
According to figure 9 it can be seen that the second pass band is significantly influenced by g_1 . In addition to g_1 , the second passage band is affected by the g_2 and g_5 and g_6 gap space. At the same time, the distance between the third and fourth stripe lines also affects the second passband.

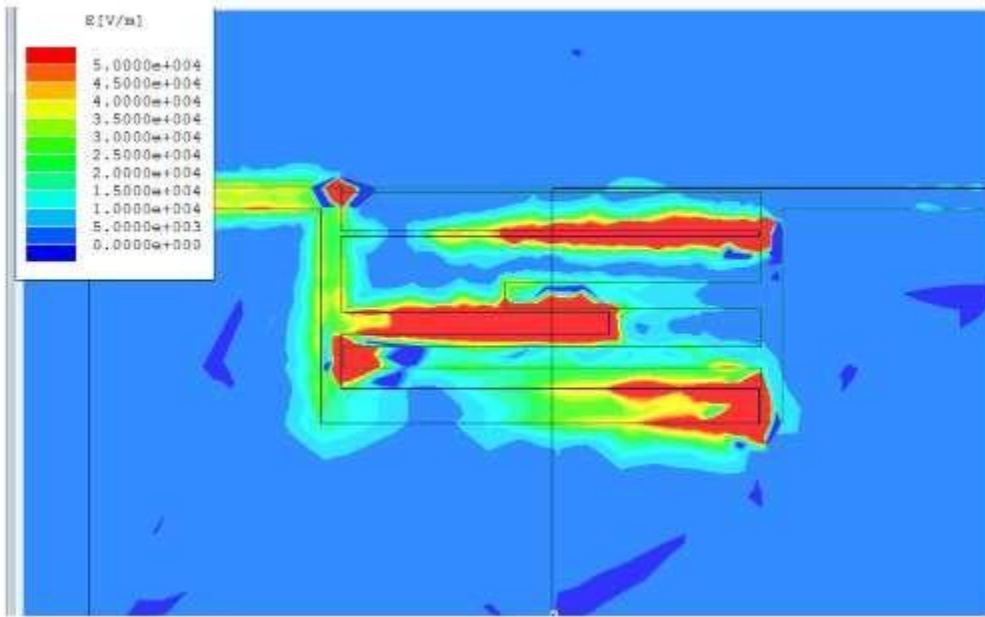


Figure 10. The electric field for $g_1 = 0.019\text{mm}$

As can be seen in figure 10, the second passband is strongly influenced by g_1 . In addition to g_1 , the second passband is affected by the g_2 and g_5 and g_6 gap space. At the same time, the distance between the third and fourth stripe lines also affects the second passband.

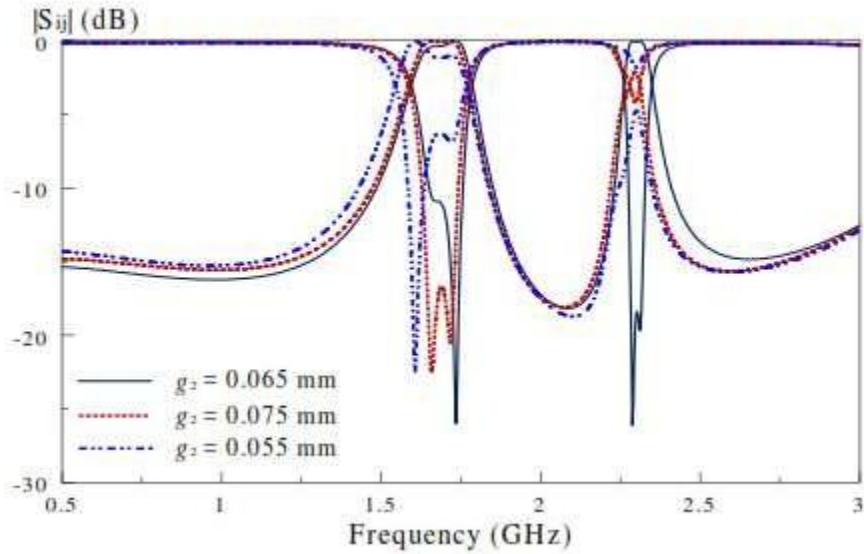


Figure 11. The Response of the Second Case

As can be seen in figure 11, the second passband is affected by the g_2 gap distance. The first passband is not very affected by the change of g_2 gap space. The optimum value of both passes is obtained at 0.065mm.

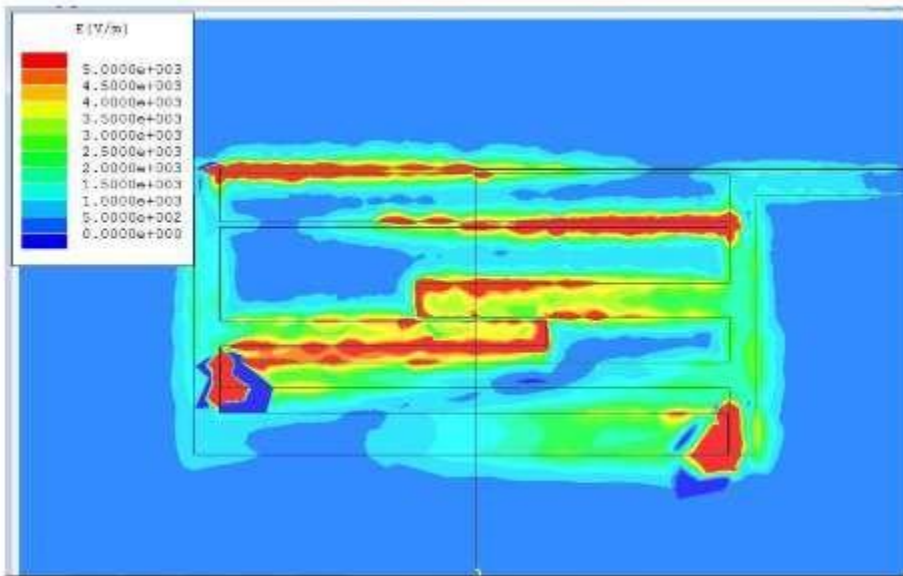


Figure 12. The electric field for $g_2 = 0.075$ mm

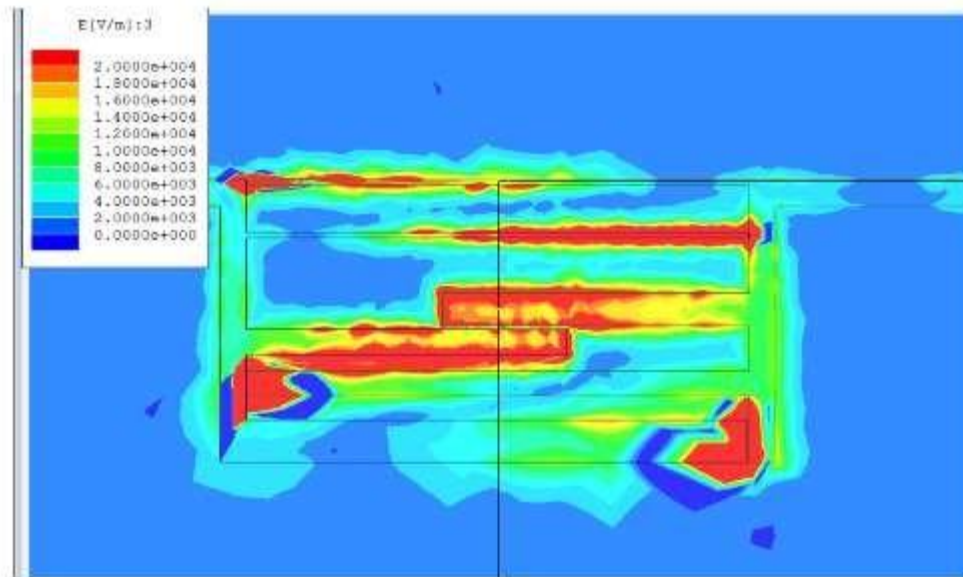


Figure 13. Electric field for $g_2 = 0.055$ mm

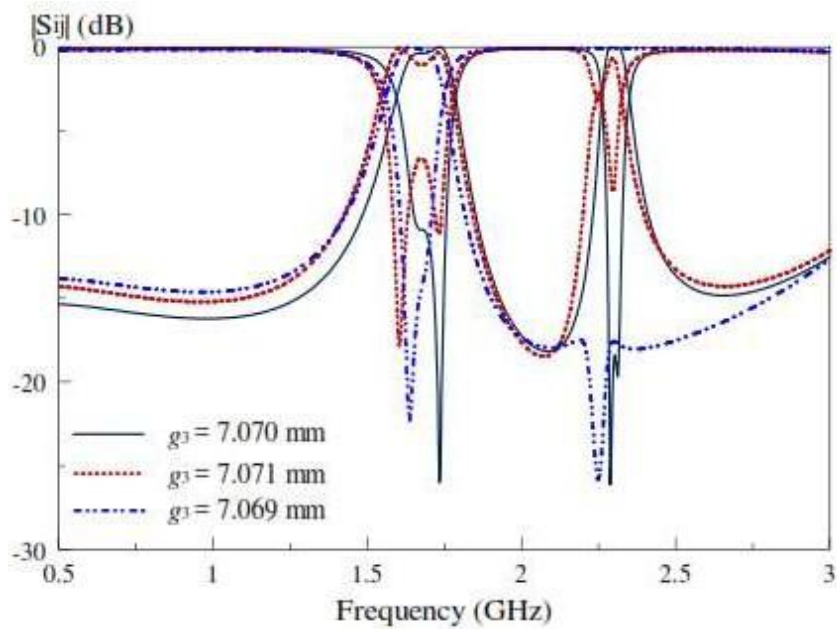


Figure 14. The Response to the Third Case

As shown in figure 14, the second pass band in $g_3 = 7.071\text{mm}$ fails faster. When the gap distance is 7.069mm , the second passband will not be badly damaged. Therefore, both transition paths are at 0.065mm in optimum mode.

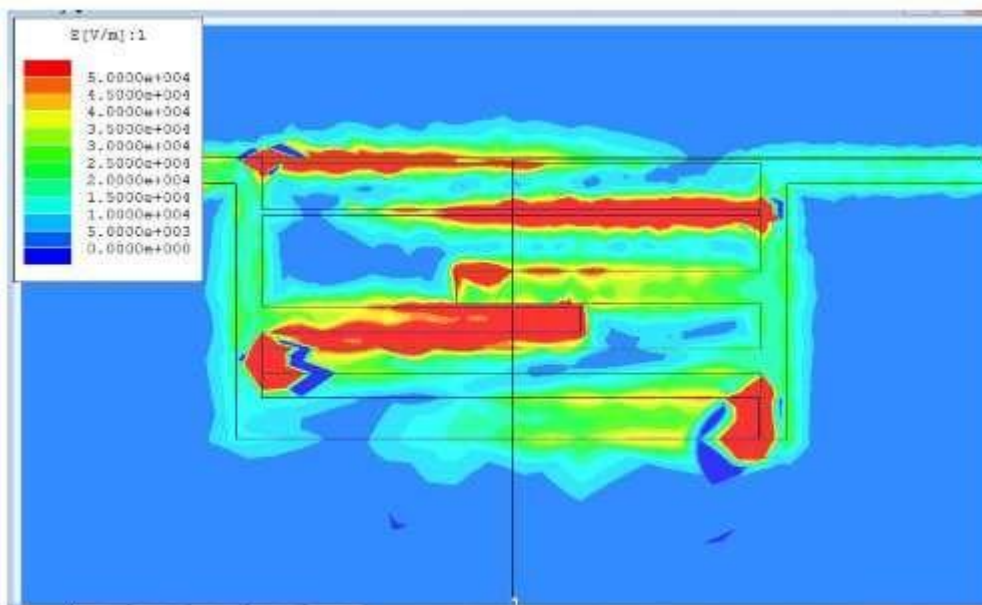


Figure 15. Electric field for $g_3 = 7.071\text{mm}$

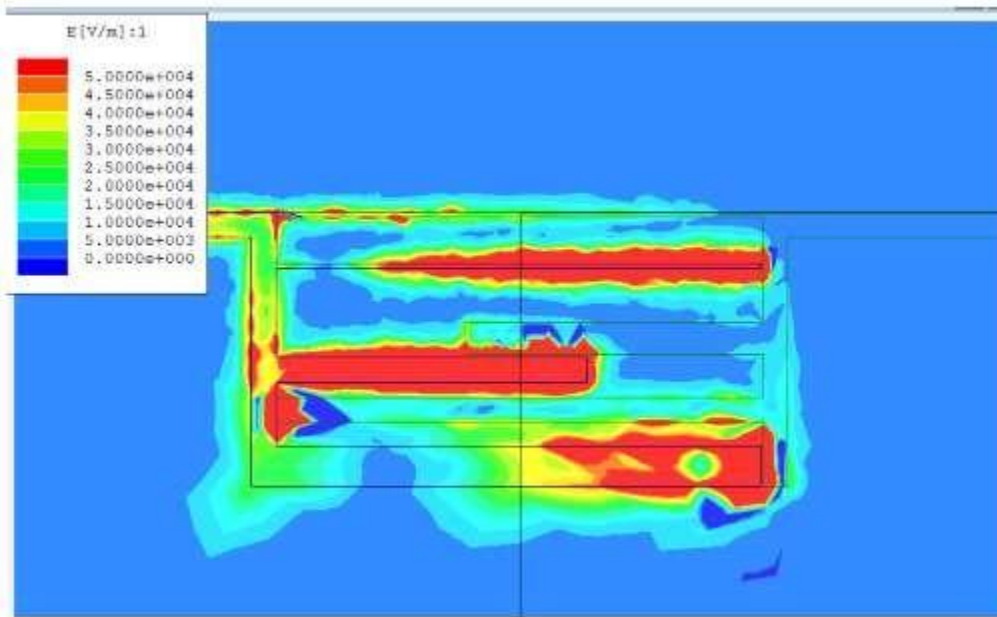


Figure 16. Electric field for $g_3 = 7.069\text{mm}$

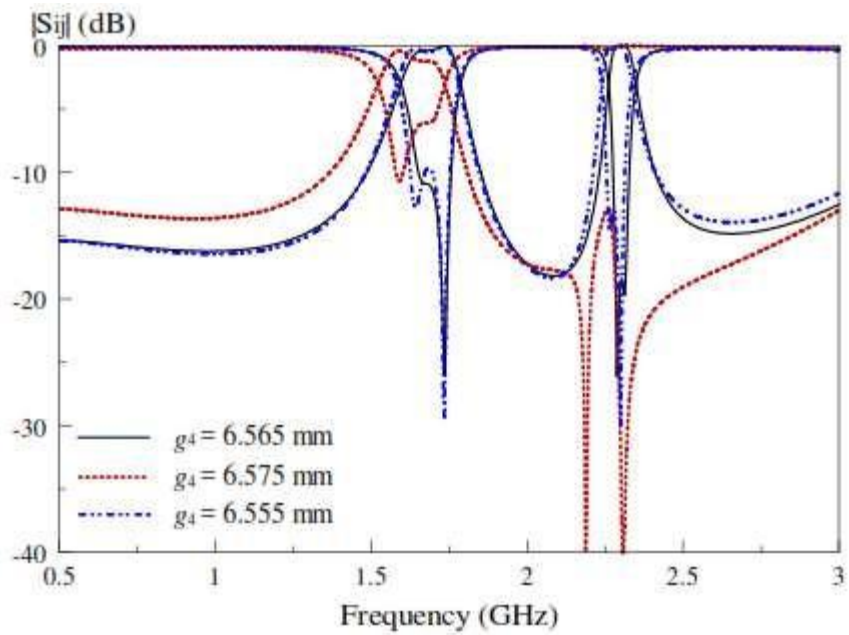


Figure 17. The Response to the Fourth Case

As can be seen in figure 17, the first and second passband will fail for $g_4 = 6.575\text{mm}$ faster. When the distance is 6.565mm , the first and second passband will be less affected.

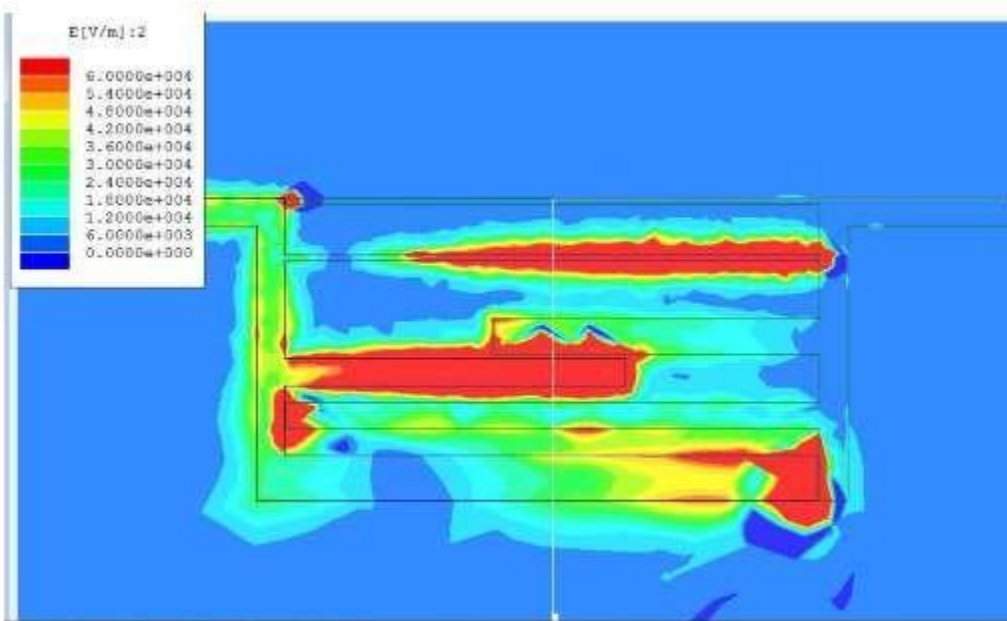


Figure 18. Electric field for $g_4 = 6.575\text{mm}$

Conclusion. In this study, the microstrip filters between two-band two-way transitions were numerically investigated using HFSS software. For validation, numerical simulation results of numerical values are validated with existing empirical data. Since the chat affects the filter hole, the filter response changes by 0.01mm. For the various examples, the effect of the chat interval was numerically investigated, and the rejection of each mode was the optimal value of the chat.

References

1. S. Yang, L. Lin, J. Chen, K. Deng, and C. H. Liang, "Design of compact dual-band bandpass filter using dual-mode stepped-impedance stub resonators," *Electronics letters.*, vol. 50, no. 8, pp. 611-613, April. 2014.
2. X. Y. Zhang, J. X. Chen, Q. Xue, and S. M. Li, "Dual-band bandpass filters using stubloaded resonators," *IEEE .Microw. Wireless Compon. Lett.*, vol. 17, No.8, pp. 583-585, Aug. 2007.
3. M. Zhou, X. Tang, and F. Xiao, "Compact dual-band bandpass filters using novel e-type resonators with controllable bandwidths", *IEEE .Microw. Wireless Compon. Lett.*, vol. 18, No.12, pp. 779-781, Dec. 2008.
4. Bin Yu, Baofu Jia and Zhaojun Zhu, "Compact tri-band bandpass filter with stub loaded stepped impedance resonator", *Electronics letters.*, vol. 51, no.9, pp. 7011-7033, April. 2015.
5. S. B. Zhang and Zhu, "Fully canonical dual-band bandpass filter with $\lambda/4$ stepped impedance resonators", *Electronics letters.*, vol. 50, no. 3, pp. 192-194, Feb. 2014.
6. S. B. Zhang and L. Zhu, "Synthesis design of dual-band bandpass filters with $\lambda/4$ stepped impedance resonators", *IEEE Trans. Microw. Theory Tech.*, vol. 61, no. 12, pp. 1812-1819, May. 2013.
7. Lin, S. -C., "Microstrip dual/quad-band filters with coupled lines and quasi-lumped impedance inverters based on parallel-path transmission", *IEEE Trans. Microw. Theory Tech.*, vol. 59, no. 8, pp. 1937-1946, 2011.
8. Zhang, S., Zhu, L., "Compact tri-band bandpass filter based on resonators with u-folded coupled-line", *IEEE .Microw. Wireless Compon. Lett.*, vol. 23, No.5, pp. 258-261, 2013.
9. Heng, Y., Guo, X., Cao, B., Wei, B., Zhang, X., Zhang, G., and Song, X., "Compact superconducting dual-band bandpass filter by combining bandpass and band-stop filters" , *Electronics letters.*, vol. 49, no.19, pp. 1230-1232, 2013.
10. W. Feng, L. Gu, W. Che and H. Chen, "Tri-band Microstrip Bandpass Filter Using Input/Output Cross Coupling," *Journal of Electromagnetic Waves and Applications.*, pp. 405-409, 2013.
11. A. Neghar, O. Aghzot, A. V. Alejos, M. G. Sanches and M. Essaïdi, "Design of Compact Multiband Bandpass Filter with Suppression of Second Harmonic Spurious by Coupling Gap Reduction," *Journal of Electromagnetic Waves and Applications.*, pp. 1813-1828, 2015.
12. Ahmed, Emad S. "Dual-Mode Dual-Band Microstrip Bandpass Filter Based on Fourth Iteration T-Square Fractal and Shorting Pin." *Radioengineering* 21.2 (2012).